

18. S. C. Gill, S. E. Weitzel, P. H. von Hippel, *J. Mol. Biol.* 220, 307 (1991).
19. A rapid procedure called "equilibrium filtration" was developed to assess theophylline binding by oligonucleotides. These assays were performed by the addition of [¹⁴C]theophylline and RNA at indicated concentrations to a 150- μ l reaction mixture containing 100 mM Hepes (pH 7.3), 5 mM MgCl₂, and 50 mM NaCl. Each binding mixture was incubated for 5 min at 25°C. The mixture was then placed in a Microcon 10 filtration device (Amicon) and centrifuged for 4 min at 13,000g, allowing 40 μ l of solution to flow through the membrane. Similar to equilibrium dialysis, the solution that remained above the molecular-weight cutoff membrane contains free theophylline, free RNA, and RNA-bound theophylline, and the filtrate contains only free theophylline at an equivalent concentration to the free theophylline in the initial solution. A 25- μ l sample was removed from each side of the filter, and the radioactivity was determined by scintillation counting. Bound theophylline was determined by the difference between the theophylline concentration of the filtrate and the theophylline concentration of the retentate. Data were fit by a least squares analysis to a standard quadratic binding equation (18) for the observed 1:1 stoichiometry. Equilibrium dialysis was also used to measure binding of theophylline and yielded dissociation constants within a factor of 2 of those obtained by equilibrium filtration.
20. Equilibrium filtration assays were performed by the addition of various concentrations of the potential competitor to 1 μ M [¹⁴C]theophylline and 3.3 μ M TCT-8 RNA in a 150- μ l reaction mixture containing 100 mM Hepes (pH 7.3), 5 mM MgCl₂, and 50 mM NaCl. Competition data were fit by a standard competition equation and fitting procedure (18) with a 1:1 stoichiometry of competitor to RNA. A K_d of 0.45 μ M for theophylline binding to RNA was used.
21. P. Plateau and M. Gueron, *J. Am. Chem. Soc.* 104, 731 (1982).
22. We thank C. Tuerk, D. Zichi, D. Parma, N. Janjic, D. McGee, W. Pieken, B. Eaton, K. Yamamoto, and L. Gold for thoughtful comments on this work and D. Bridon for synthesis of theophylline compounds. This work was partially supported by NIH grant AI33098 and an NIH Research Career Development Award (AI01051) to A.P. The 500-MHz NMR spectrometer was purchased with partial support from NIH grant RR03283. A.P. also thanks the W. M. Keck Foundation for their generous support of RNA science on the Boulder campus.

6 December 1993; accepted 24 January 1994

Channel-Like Function of the Na,K Pump Probed at Microsecond Resolution in Giant Membrane Patches

Donald W. Hilgemann

Ion transporters can be thought of as ion channels that open and close only at one end at a time. As in real channels, ions may cross through an electrical field as they diffuse into and bind within the transporter pore, thereby generating electrical current. Extracellular sodium binding by the sodium potassium (Na,K) pump is associated with ultrafast charge movements in giant cardiac membrane patches. The charge movements are complete within 4 microseconds. They occur only when binding sites are open to the extracellular side, and they are abolished by ouabain and by the removal of extracellular sodium. Fast extracellular ion binding may be the exclusive source of Na,K pump electrogenicity.

The adenosine triphosphate (ATP)-driven Na,K pump, or Na,K adenosine triphosphatase, extrudes three Na ions in exchange for two K ions and therefore generates an electrical current (1) (Fig. 1A). Recently, it was proposed that the immediate source of electrogenicity in the Na,K pump cycle is the binding and dissociation of Na from an "access channel" open to the extracellular side (2) (step 4 of Fig. 1A). This proposal explains neatly why changes of extracellular Na and membrane potential appear equivalent in Na flux studies (2) and why extracellular Na inhibits pump activity in a voltage-dependent manner (3, 4). However, important kinetic predictions have not been verified. Most importantly, when binding sites are open to the extracellular side ("E₂" conformation), it should be possible to record ultrafast charge movements related to Na binding and dissociation. Similar proposals and considerations apply equally to a number of other transporters (5).

The giant cardiac membrane patch technique (6) is well suited to test such predictions, because it allows a fast (4 μ s) voltage clamp of a large membrane area (~10 pF) with ~1000 Na,K pump sites per square micrometer. To facilitate both the identifi-

cation and quantification of fast charge movements, charge transfer per se is recorded directly through an integrating patch-clamp amplifier. The charge transfer signals thus represent the time integral of membrane current, and membrane current is their first derivative. The protocols used may be derived from Fig. 1A, which illustrates the simplest possible access-channel model of the Na,K pump; Fig. 1B illustrates a refined model of Na release that will be outlined with experimental results.

The charge movements (7) are recorded in the absence of K to prevent pump cycling (that is, steps 5 to 8 in Fig. 1A). In the additional absence of cytoplasmic Na and ATP, the pump orients to a configuration with empty binding sites open to the cytoplasmic side ("E₁" conformation). Voltage pulses are first applied under this base line condition, whereby transitions to the other illustrated pump states are not possible. Either Na or ATP can be applied individually to the cytoplasmic side without any clear changes of base line signals, indicating that cytoplasmic Na binding (step 1) is not strongly electrogenic (8, 9). When Na and ATP are applied together, however, the pump is phosphorylated and the transporter pore closes from the cytoplasmic side, thereby "occluding" Na within the pump (step 2). The subsequent reactions (steps 3 and 4)

include electrogenic steps (9), and they can then be driven back and forth by changes of membrane potential (dotted field). The corresponding charge movements (3, 10) are isolated by the subtraction of records in the absence of cytoplasmic Na, ATP, or both from records in the presence of cytoplasmic Na and ATP (11).

Typical Na,K pump charge movements are shown in Fig. 2A, with the use of voltage steps from 0 mV to the different indicated potentials (-250 to +150 mV in 50-mV intervals; 10 mM cytoplasmic Na, 120 mM extracellular Na, no other monovalent cations, 0.4 mM ATP) with subtraction of the base line signals without ATP (12). Slow components over 2 to 6 ms (Q_{slow}) dominate the records, and fast components (Q_{fast}) appear as initial charge jumps in the first 100 μ s during voltage steps. The Q_{slow} components can all be fitted to single exponential functions that are plotted with each record as a dashed line. The exponentials are hardly visible outside signal noise, suggesting that the time course of individual Q_{slow} components may be determined by a single reaction. The rate constants of Q_{slow} (" k_{slow} "; Fig. 2B) decrease to a minimum at positive potentials [as in (3, 10)], ~400 s⁻¹ in these records at 37°C. They appear to saturate toward a maximal value with hyperpolarization, and their voltage dependence can be described by a Boltzmann function (midpoint, -170 mV; slope, 0.74, appropriate for movement of one charge through 74% of the membrane field). Complete saturation at negative potentials was found when the initial rates were examined from -50 to -400 mV during 0.4-ms voltage pulses. The rate of Q_{slow} (as well as its magnitude) already reaches a maximum value at -150 mV when extracellular Na is increased to 180 mM.

The fact that the reaction rates of Q_{slow} saturate at both extremes of potential and are dependent on extracellular Na suggests that a fast, electrogenic Na binding reaction may be "sandwiched" between (that is,

Department of Physiology, University of Texas Southwestern Medical Center at Dallas, 5323 Harry Hines Boulevard, Dallas, TX 75235, USA.

in series with) two voltage-independent processes. This order is accounted for in the model of Fig. 1B [refined from an "electrostatic" model (13)] by the assumption that the Na binding sites open to the extracellular side in two voltage-independent steps. First, binding sites open to form a channel-like pathway (E_2P3N) through which the first of the three Na ions can escape in the major electrogenic event (14). Then, binding sites open wider in the second reaction, causing membrane potential to shift across both the bound ions and binding sites. Assuming that binding site charge is close to -2 (9), this reaction is electroneutral. The last two Na ions can then dissociate from the E_2P2N state in reactions that are only weakly voltage-dependent.

The amplitudes of Q_{slow} charge movements are nearly equal for voltage steps away from 0 mV ("on" direction) and back to 0 mV ("off" direction; Fig. 2B) (Boltzmann midpoint, -45 mV; slope, 0.67). The near equality of on and off charge movements over the large voltage range of these experiments clearly contradicts the simple access-channel model illustrated in Fig. 1A. If the entire E_2 pump existed as an access channel, a discrepancy between on and off charge movements would develop with increasingly more negative voltage steps. At very negative potentials, Na would occupy all channel sites in a fast initial charge jump, thereby precluding any slow charge movement during subsequent reactions affecting binding site availability. During the corresponding depolarizing step, all charge movement would occur exclusively in a slow phase as binding sites open and Na dissociates.

The refined model accounts readily for the results by assuming that the channel-like state (E_2P3N) is a transitional, high-energy state with a very short "open time" (transition rates b and $c \gg a$ and d). E_2P3N then never accumulates to a significant extent and cannot support a significant fast charge movement. With strong depolarization, the electrogenic release of Na from the E_2P3N state is rate-limited by the voltage-independent transition, a , from the E_1P3N state. With strong hyperpolarization, the electrogenic binding of Na is rate-limited by the voltage-independent transition, d , from the E_2P2N state to the E_2P3N state. The fast charge movements that are observed probably reflect the weakly voltage-dependent binding and unbinding of Na to and from the E_2P2N state (Fig. 3).

In Fig. 3, the fast charge movements observed (Q_{fast}) are examined at $4\text{-}\mu\text{s}$ resolution. Before the records in Fig. 3A were taken, a pre-pulse to $+100$ mV was applied for 10 ms, and then the indicated protocol of $50\text{-}\mu\text{s}$ voltage steps to more negative potentials was applied. First, voltage steps

were applied in increasing magnitude from $+50$ to -200 mV; then, a capacitance reset was performed at the arrow, and the same steps were applied in reverse order. Identical results were obtained by the subtraction of the base line records after the removal of cytoplasmic Na (as in Fig. 3A) or after the

removal of cytoplasmic ATP. The charge transfer reactions are entirely complete within the $4\text{-}\mu\text{s}$ resolution of the present instrumentation (Fig. 3B). The voltage dependence of the fast charge movements (Fig. 3C) is remarkably shallow (Boltzmann slope, 0.26), and results are similar when

Fig. 1. Possible sources of electrogenicity in the Na,K pump cycle. The pump cartoons are all oriented with the extracellular side pointing upward. Filled circles represent Na ions, open circles represent K ions, and P represents the covalently bound phosphate that is donated by ATP upon phosphorylation. (A) Access channel model of the pump cycle in which both Na (2) and K (18) pass through a channel-like structure upon binding. The numbers 1 to 8 indicate the major steps in the pump cycle. Ion binding reactions, which are assumed to be extremely fast in relation to other steps, are represented by double-headed arrows. In this report, the terms E_1 and E_2 designate states with binding sites open to the cytoplasmic and extracellular sides, respectively. Step 1: Na binds on the cytoplasmic side. Step 2: The pump is phosphorylated and cytoplasmic Na is occluded. Step 3: Binding sites open to the extracellular side. Step 4: Na is released to the outside, generating an outward charge movement. Step 5: K binds on the extracellular side, generating an inward charge movement. Step 6: The pump is dephosphorylated, and K is occluded. Step 7: The K binding site opens to the cytoplasmic side. Step 8: K is released to the cytoplasm. The dotted field encloses the reactions that can take place during charge movement measurements in the absence of K. (B) Refined model of Na release from the Na,K pump [compare with (13)]. The E_1P3N state contains three occluded Na ions. In a first opening reaction to the extracellular side, the E_2P3N state is formed, from which one Na ion can rapidly dissociate (and rebind) in the major electrogenic step. Binding sites open further in a second reaction, thereby shifting membrane electrical field across the last two Na ions and their binding sites. For this process to be electroneutral, net binding-site charge must be close to -2 (9). The second and third Na ions can then dissociate (and rebind) from the E_2P2N state across only a small electrical distance (8, 13), and K ions subsequently bind with similarly weak voltage dependence.

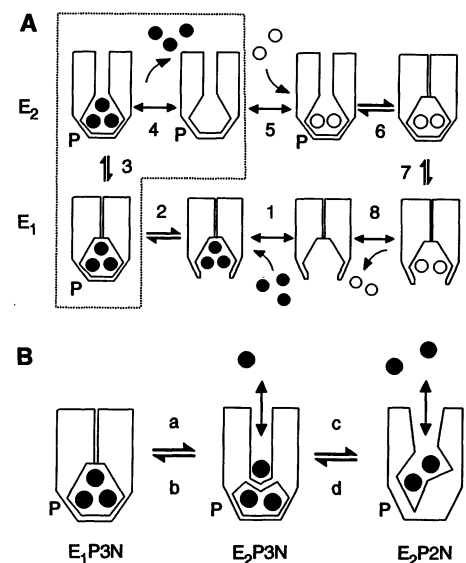
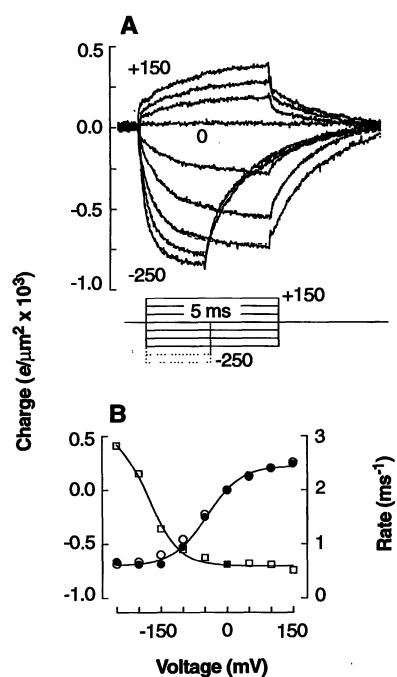


Fig. 2. Charge movements of Na translocation by the Na,K pump in a giant cardiac-membrane patch. Charge transfer, the time integral of membrane current, is recorded directly from an integrating patch-clamp amplifier. Records presented are a subtraction of records in the absence of cytoplasmic ATP from records in the presence of 0.4 mM cytoplasmic ATP and 10 mM cytoplasmic Na. Extracellular Na is 120 mM. The records are low pass-filtered at 5 kHz. (A) From top to bottom, Na,K pump charge movement for 5-ms voltage pulses from 0 to $+150$, $+100$, $+50$, 0 , -50 , -100 , and -150 mV; and for 2.5-ms voltage pulses from 0 to -200 and 250 mV. The calibration is made on the assumption of a specific membrane capacitance of 0.8 $\mu\text{F}/\text{cm}^2$. Dotted lines, barely visible outside of signal noise, plot the best fit of each record to a single exponential function starting 100 μs after the voltage step. (B) Open squares give rate constants (k_{slow}) of the fitted exponentials from (A). The value at 0 mV (filled square) is the mean value for the eight relaxation curves at 0 mV; standard error was within the symbol size. The fitted Boltzmann function has a midpoint of -170 mV and a slope of 0.74 . Filled circles give amplitudes of the fitted charge movements (Q_{slow}) during the on voltage steps in (A), and open circles give values for the return, off, pulses to 0 mV. The fitted Boltzmann slope is 0.68 .



extended voltage protocols are used (12 observations).

That these signals represent electrogenic binding of Na by the Na,K pump is supported by four findings: First, the signals are completely absent when the same protocols are performed with 100 μ M ouabain in the pipette. Second, the magnitudes of Q_{fast} for any fixed voltage step show a steep dependence on holding potential (Q_{fast} in Fig. 3D; Boltzmann slope, 1.1), similar to the overall slow charge transfer process that deter-

mines the availability of extracellular binding sites (circles in Fig. 2B). Third, the ability to evoke fast charge movements is entirely lost when Na is omitted from the pipette (Fig. 3E). And fourth, the magnitude of fast charge transfer for potential jumps from +50 to -50 mV shows a bell-shaped dependence on extracellular Na, declining at high extracellular Na, as expected for saturation of the binding sites (Fig. 3E) (K_d , 30 mM at +50 mV).

These same characteristics provide the

evidence that Q_{fast} reflects Na binding and unbinding mostly from E_2P_2N , rather than from E_2P_3N . First, Q_{fast} is maximized by depolarization (Fig. 3D), which moves the pump to the E_2P_2N state and out of the E_2P_3N state. Second, larger Boltzmann slopes must be expected for Na binding to the E_2P_3N state to account for the steepness of Q_{slow} . And third, the Na affinity of Q_{fast} is higher than expected for Na binding to E_2P_3N (Fig. 4).

Is the refined model of Na release from the Na,K pump viable? As illustrated in Fig. 4, charge movements recorded with different voltage protocols and over a wide range of extracellular Na concentrations can be reconstructed well by a single set of model parameters. To what extent, then, are the microscopic events of Na translocation by the Na,K pump really analogous to channel function? Almost nothing is known about the possible interactions of ions with (or within) ion channels when they are closed in either "deactivated" or "inactivated" states. One possibly analogous process in ion channel function is the gating of some channels by impermeant ions (15). The immediate molecular events underlying Na,K pump electrogenicity may be either the movement of Na through a static pore, as drawn for the E_2P_3N state in Fig. 1B, or fast conformational changes associated with ion binding and binding site dehydration. Further refinement of the giant patch techniques should greatly facilitate studies of these and related fast molecular events relevant to the microscopic function and structure of ion transporters and channels (20).

REFERENCES AND NOTES

1. P. Läuger, *Electrogenic Ion Pumps* (Sinauer, New York, 1991).
2. D. C. Gadsby, R. F. Rakowski, P. De Weer, *Science* **260**, 100 (1993).
3. M. Nakao and D. C. Gadsby, *Nature* **323**, 628 (1986).
4. R. F. Rakowski, D. C. Gadsby, P. De Weer, *J. Gen. Physiol.* **93**, 903 (1989).
5. P. Mitchell and J. J. Moyle, *Biochem. Soc. Spec. Publ.* **4** (1974), p. 91; G. Althoff, H. Lill, W. J. Junge, *J. Membr. Biol.* **108**, 263 (1989); L. Lagnado, L. Cervetto, P. A. McNaughton, *Proc. Natl. Acad. Sci. U.S.A.* **85**, 4548 (1988); D. D. Loo, A. Hazama, S. Supplisson, E. Turk, E. M. Wright, *ibid.* **90**, 5767 (1993); D. W. Hilgemann, D. A. Nicoll, K. D. Philipson, *Nature* **352**, 715 (1991); S. Mager *et al.*, *Neuron* **10**, 177 (1993).
6. D. W. Hilgemann, *Pflügers Arch.* **415**, 247 (1989); A. Collins, A. V. Somlyo, D. W. Hilgemann, *J. Physiol.* **454**, 27 (1992).
7. Giant patches were formed and excised from guinea pig myocytes as described in (6). Pipette tip diameters were 25 to 30 μ m (<100 kilohms), and membrane capacitance was 8 to 12 pF. The pipette ends were wrapped with a highly viscous mixture of Parafilm and mineral oil to negate any capacitance changes with solution changes. Cells were dispersed into a K-free solution before seal formation. An Axopatch 200 capacitance-feedback patch clamp (Axon Instruments, Foster City, CA) was used with direct digital acquisition of the charge transfer signal at 50 kHz to 10 MHz.

Fig. 3. Ultrafast charge movements of extracellular Na binding by the Na,K pump. (A) After a 10-ms voltage step to +100 mV, 50- μ s voltage pulses were applied in 50-mV increments to -200 mV, followed by a 250- μ s pause during which the capacitance feedback of the patch clamp was reset (arrow). Thereafter, the same series of voltage steps was applied in reverse order. Five records were averaged in the absence of cytoplasmic Na and were subtracted from the average of five records in the presence of 5 mM cytoplasmic Na and 0.4 mM ATP. (B) Unfiltered records, averaged 50 times, with the same pre-pulse and conditions as in (A). Step hyperpolarization from +100 to -100 mV for 50 μ s, with subtraction of the records in the absence of cytoplasmic Na. Calibration is in femtocoulomb (fC). (C) Voltage dependence of the fast charge movement (Q_{fast}). Open circles are the average values for the two protocols used in (A). Results were identical for the subtraction of records in the absence of ATP. Closed circles give equivalent data from a data set extended to +200 mV. The fitted Boltzmann function has a slope of 0.26 and a midpoint of -3.5 mV. The numbers 0 and 1 represent the minimum and maximum, respectively, of the fitted Boltzmann functions. (D) The maximum fast charge movement (+100 to -200 mV) obtained within 75 μ s after the membrane potential was held for 10 ms at different potentials from -120 mV to +120 mV (Q_{fast}). The fitted Boltzmann function has a slope of 1.2 and a midpoint of -32 mV. (E) Extracellular Na dependence of the fast charge movement (Q_{fast}) from +50 to -50 mV. No fast or slow charge movement could be recorded with 0 extracellular Na. However, a small steady-state current developed, thought to be a proton current, which is similar to the results of others (19). The fitted curve assumes that membrane depolarization reduces the effective Na concentration available to a binding site by a fixed fraction at all Na concentrations. The fitted K_d for the binding site is 30 mM.

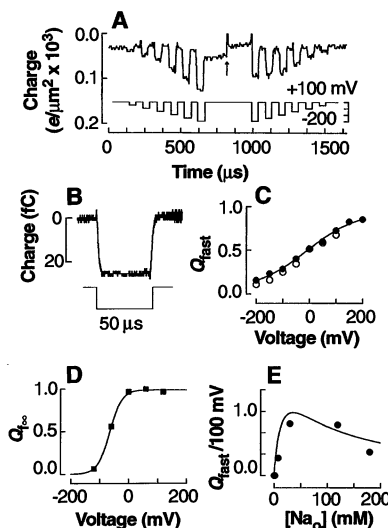
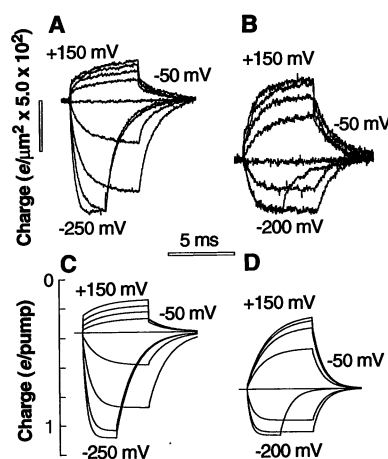


Fig. 4. (A and B) Na,K pump charge movements and (C and D) their simulated counterparts with (A and C) 18 mM and (B and D) 180 mM extracellular Na. Filter frequency, 5 KHz. Results in (A) and (B) are from different patches. Very consistent results were obtained in 16 stable patches with seven different extracellular Na concentrations used from 2 to 180 mM. Holding potential is -50 mV, and voltage pulses are in increments and decrements of 50 mV. For clarity, the -250-mV record is not included in (B); both the magnitudes and rates of Q_{slow} are saturated already at -150 mV. The voltage dependencies of both the Q_{slow} charge movements and their rates are shifted by about 60 mV with the 10-fold change of extracellular Na used here. To simulate these results with the model of Fig. 1B, most parameters could be based directly on the experimental results. The calibration (charge) gives the average number of net elementary charges, which have apparently moved across the entire membrane field in each pump molecule. The rate constants a, b, c, and d were 0.64, 24, 40, and 4 ms^{-1} , respectively. The dissociation constant for Na binding in the E_2P_3N state was 2 M over an electrical distance of 80% of the membrane field; the affinity must be very low to explain the shifts of charge movements and their rates with changes of extracellular Na over the range of 180 to 18 mM. For the E_2P_2N state, the binding of two Na ions was lumped as a single reaction (dissociation constant, 20 mM) over an electrical distance of 30% of the membrane field.



- The temporal resolution of the voltage clamp (4 μ s) is limited by the rise time of the voltage pulse step applied to the amplifier. The capacitance feedback was reset just before the onset of all signals presented. A small, rising slope in charge transfer records, corresponding to a steady-state current, was subtracted from all records presented. This current probably corresponds to a low rate of pump cycling during which three cytoplasmic Na ions are exchanged for two extracellular Na ions (16). All results were obtained at 37°C. Membrane capacitance was determined as the difference between pipette capacitance with the intact membrane patch and the capacitance after patch rupture with subsequent formation of a hydrocarbon (hexane) meniscus, about 1 μ m in thickness, across the pipette orifice. The extracellular (pipette) solution contained 120 mM Na-[2-(*N*-methylol)ethanesulphonic] acid (MES), 0.5 mM MgCl₂, 15 mM *N*-methylglucamine (NMG)-Cl, 10 mM tetraethylammonium (TEA), 10 mM MES, 5 mM EGTA, and 15 mM Hepes, set to pH 7.0 with additional NMG. For the cytoplasmic solution and for pipette solutions with varied Na concentrations, Na-MES was replaced with NMG-MES.
8. W. Stürmer, R. Bühler, H.-J. Apell, P. Läuger, *J. Membr. Biol.* 121, 163 (1991).
 9. R. Goldshleger, S. J. D. Karlsh, A. Rephaeli, W. D. Stein, *J. Physiol.* 387, 331 (1987); K. Fendler, E. Grell, E. Bamberg, *FEBS Lett.* 224, 83 (1987).
 10. R. F. Rakowski, *J. Gen. Physiol.* 101, 117 (1993).
 11. All Na,K pump charge movements defined in this way were completely absent when 100 μ M ouabain was included in the pipette (that is, on the extracellular side). With 120 mM extracellular Na, 1 μ M ouabain completely abolished charge movements.
 12. Nearly identical results were obtained by the subtraction of signals after the removal of cytoplasmic Na. Very similar results were also obtained when high cytoplasmic PO₄ (4 mM) and Mg (4 mM) were applied to induce the E₂ pump conformation, and records taken after the removal of PO₄ were subtracted.
 13. S. Heyse, I. Wuddel, H.-J. Apell, W. Stürmer, *J. Gen. Physiol.*, in press.
 14. This process requires that the membrane electrical field falls off along the diffusion pathway of the Na ion (that is, the access channel). The position and profile of the membrane field along such a channel, closed at one end, depend minimally on the unknown physical (dielectric) properties of the membrane protein and the geometry of the pore. It seems safe to assume that if the pore is so narrow that water is structured (or bound) within the pore, then membrane potential will fall off along its length. This relation can be assumed for the E₂P3N state. If the channel is wider and the dielectric properties of the transporter protein are

- more like those of membrane than of water, then the electrical field will be forced out of the water-filled pore and into a position through its closed end. This relation can be assumed for the E₂P2N state.
15. C. A. Vandenberg, *Proc. Natl. Acad. Sci. U.S.A.* 84, 2560 (1987); L. Nowak, P. Bregestovski, P. Ascher, A. Herbet, A. Prochiantz, *Nature* 307, 462 (1984).
 16. K. H. Lee and R. Blostein, *Nature* 285, 338 (1980).
 17. D. W. Hilgemann, K. D. Philipson, D. A. Nicoll, *Biophys. J.* 61, A390 (1992).
 18. L. A. Vasilets and W. Schwarz, *J. Membr. Biol.* 91, 43 (1990).
 19. R. F. Rakowski, L. A. Vasilets, J. La Tona, W. Schwarz, *ibid.* 121, 177 (1991).
 20. I thank G. A. Frazier and Texas Instruments for designing and building the data acquisition-pulse generator system used in these experiments; R. Lobdill and Axon Instruments for advice and modifying the patch clamp used; P. Foley for technical assistance; V. V. Golobov for mathematical advice; and D. C. Gadsby, R. A. Levis, M. Weber, S. Matsuoka, and K. D. Philipson for helpful discussions. Supported by grants from the American Heart Association and the National Institutes of Health. This work has been reported in part in abstract form (17).

20 October 1993; accepted 14 January 1994

Crystal Structures at 2.5 Angstrom Resolution of Seryl-tRNA Synthetase Complexed with Two Analogs of Seryl Adenylate

Hassan Belrhali, Anna Yaremchuk, Michael Tukalo, Kjeld Larsen, Carmen Berthet-Colominas, Reuben Leberman, Barbro Beijer, Brian Sproat, Jens Als-Nielsen, Gerhard Grübel, Jean-François Legrand, Mogens Lehmann, Stephen Cusack*

Crystal structures of seryl-tRNA synthetase from *Thermus thermophilus* complexed with two different analogs of seryl adenylate have been determined at 2.5 Å resolution. The first complex is between the enzyme and seryl-hydroxamate-AMP (adenosine monophosphate), produced enzymatically in the crystal from adenosine triphosphate (ATP) and serine hydroxamate, and the second is with a synthetic analog of seryl adenylate (5'-O-[*N*-(*L*-seryl)-sulfamoyl]adenosine), which is a strong inhibitor of the enzyme. Both molecules are bound in a similar fashion by a network of hydrogen bond interactions in a deep hydrophilic cleft formed by the antiparallel β sheet and surrounding loops of the synthetase catalytic domain. Four regions in the primary sequence are involved in the interactions, including the motif 2 and 3 regions of class 2 synthetases. Apart from the specific recognition of the serine side chain, the interactions are likely to be similar in all class 2 synthetases.

Aminoacyl-tRNA synthetases specifically attach amino acids to the 3'-adenosine of their cognate tRNAs in a two-step reaction. In the presence of Mg²⁺ and ATP, the enzyme first activates the amino acid to

form the enzyme-bound aminoacyl-adenylate intermediate. In the second step, the amino acid is ligated to the cognate tRNA. The 20 aminoacyl-tRNA synthetases are divided into two classes of ten (1, 2). The two classes are characterized by different short sequence motifs and have quite different catalytic domain topologies, the Rossmann fold for class 1 and an antiparallel β fold for class 2 (3). For class 1 synthetases, crystal structures of complexes with ATP have been described for methionyl-tRNA synthetase (MetRS) (4) and GlnRS (5), with the amino acid alone for TyrRS (6) and with the aminoacyl-adenylate for

TyrRS (7) and TrpRS (8). A catalytic pathway for the amino acid activation has been proposed for TyrRS (9) and GlnRS (10). For class 2 synthetases, preliminary results have been given for the ATP binding site (11-13), but no structural information is available for the amino acid binding site.

The crystal structures of seryl-tRNA synthetase from *T. thermophilus* complexed with two different seryl-adenylate analogs described here reveal the aminoacyl-adenylate binding site and the role of several of the conserved residues in class 2 aminoacyl-tRNA synthetases. The first complex was obtained by soaking native crystals of the enzyme with ATP and serine hydroxamate (SerHx, ⁺H₃N-HCR-CO-N(H)OH, where R is the serine side chain). SerHx inhibits growth in *Escherichia coli* and has been described as a competitive inhibitor of the enzyme toward the amino acid (14). The crystallographic data reveal strong difference electron density for a serine hydroxamate-AMP (SerHx-AMP) molecule (Fig. 1C). The enzymatic activation of serine hydroxamate has subsequently been confirmed by biochemical studies (see below). Ueda *et al.* (15) have described a synthetic alanyl-adenylate analog (5'-O-[*N*-(*L*-alanyl)-sulfamoyl]adenosine) and showed that it was an inhibitor of alanyl-tRNA synthetase activity. Following this idea, we have synthesized the corresponding seryl compound, 5'-O-[*N*-(*L*-seryl)-sulfamoyl]adenosine (Fig. 1B) and have co-crystallized it with *T. thermophilus* seryl-tRNA synthetase (16). This second structure confirms the location of the seryl-adenylate binding site and comparisons with the first structure indicate that the two analogs do not have the same length linkage

H. Belrhali, A. Yaremchuk, M. Tukalo, K. Larsen, C. Berthet-Colominas, R. Leberman, S. Cusack, EMBL Grenoble Outstation, c/o ILL, BP 156, 38042 Grenoble Cedex 9, France.

B. Beijer and B. Sproat, Biochemical Instrumentation Programme, EMBL, Meyerhofstrasse 1, Postfach 10.2209, D-69012 Heidelberg, Germany.

J. Als-Nielsen, G. Grübel, J.-F. Legrand, M. Lehmann, European Synchrotron Radiation Facility, BP 220, F-38043 Grenoble Cedex, France.

*To whom correspondence should be addressed.